 CMES, vol.40, no.2, pp.155-174, 2009

Nonlinear Micro Circular Plate Analysis Using Hybrid Differential Transformation / Finite Difference Method

Cha'o-Kuang Chen[1,2], **Hsin-Yi Lai**[1], **Chin-Chia Liu**[1]

Abstract: Electrostatically-actuated micro circular plates are used in many micro-electro-mechanical systems (MEMS) devices nowadays such as micro pumps and optical switches. However, the dynamic behavior of these circular plates is not easily analyzed using traditional analytic methods due to the complexity of the interactions between the electrostatic coupling effects. Accordingly, this study develops an efficient computational scheme in which the nonlinear governing equation of the coupled electrostatic force acting on the micro circular plate is solved using a hybrid differential transformation / finite difference approximation method. In deriving the dynamic equation of motion of the micro plate, explicit account is taken of both the residual stress within the plate and the uniform hydrostatic pressure acting on its upper surface. It is shown that the pull-in voltage increases with an increasing value of the residual stress, but reduces with an increasing hydrostatic pressure. The predicted values of the pull-in voltage are found to deviate by no more than 1.75% from those presented in the literature. Overall, the results presented in this study demonstrate that the differential transformation / finite difference method provides a computationally efficient and precise means of obtaining detailed insights into the nonlinear behavior of the micro circular plates used in many of today's MEMS-based actuator systems.

Keywords: Pull-in voltage; Micro circular plate; Electrostatic actuator; Hybrid Method; Differential Transformation

1 Introduction

In recent years, micro-electro-mechanical systems (MEMS) devices have been increasingly deployed for a wide range of applications in the pharmaceutical, medical, food-processing, fluidic control, transportation, and telecommunications fields.

[1] Department of Mechanical Engineering, National Cheng Kung University, Tainan, Taiwan
[2] Corresponding author. Tel.: +886-6-2757575 ext. 62140; Fax: +886-6-2342081; E-mail: ckchen@mail.ncku.edu.tw

Typical applications include micro-scale actuators for use in the aerospace and medical fields [Son, Lal, Hubbard and Olsen (2001)], electrostatic micro-mirror actuators for fiber-optic switching systems [M. Hu, H. Du, S. Ling, B. Liu and G. Lau (2005)], thermo-pneumatic micro-pumps for fluid supply systems in the biological field [Bustgens, Bacher, Menz and Schomburg (1994)], and so on. The actuation systems used in today's MEMS devices can be broadly classified as either electrostatic [Ye and Mukherjee (2000)], thermal, piezoelectric [Rezazadeh, Tahmasebi and Zubstov (2006)] or electromagnetic [Luharuka, LeBlanc, Bintoro, Berthelot and Hesketh (2008)]. Of these various techniques, electrostatic actuation schemes are commonly preferred since they are easily fabricated using established surface micromachining techniques, have a rapid response and a low power consumption. In practice, the actuation effect in such schemes is created by generating an electrostatic force between the stationary and the moving parts of the actuator through the application of an external voltage. However, in implementing such a system, great care must be taken in specifying the the device parameters and operating conditions in order to prevent the so-called "pull-in phenomenon", in which the attractive electrostatic force induced by the external voltage exceeds the restoring force developed within the deflected membrane and therefore causes it to collapse and to make momentary contact with the lower electrode [Osterberg and Senturia (1997)].

The pull-in phenomenon has attracted extensive attention in the literature. For example, Bettini [Bettini, Brusa, Munteanu, Specogna and Trevisan (2008)] analyzed the nonlinear pull-in behavior of electrostatic microactuators using sequential and non-incremental finite element (FE) methods and a discrete geometric approach, respectively. Duan [Duan and Wan (2007)] performed one- and two-dimensional analyses of the pull-in behavior of the thin film within a RF switch. Wang [Wang, Li and Lam (2007)] presented a meshless point-weighted least-squares (PWLS) method for the analysis of MEMS devices, and demonstrated its use in analyzing the pull-in phenomenon in typical electrostatically-actuated devices.

In most electrostatically-actuated MEMS devices, the deformable, upper electrode has the form of a thin circular plate. In this paper, the micro circular plate actuation system is modeled as an equivalent parallel plate capacitor with clamped edges. In modeling the dynamic behavior of the actuation system, it is assumed that that a linear uniform hydrostatic pressure acts on the upper surface of the plate and a nonlinear electrostatic force induced by an externally-applied voltage acts between the lower surface of the plate and the fixed substrate (see Fig. 1). In theory, the dynamics of the micro circular plate can be analyzed using three different actuation models. For example, the effects of the hydrostatic pressure in creating an initial displacement of the plate can first be considered, and an electrostatic force then

applied to drive the plate toward the lower substrate. Alternatively, the hydrostatic pressure can be regarded as an additional actuation force which acts on the circular plate once it has already been deflected to a certain initial position under the effects of an initial electrostatic force. Finally, an assumption can be made that the hydrostatic pressure and the electrostatic force act in concert in driving the circular plate toward the lower electrode [Nabian, Rezazadeh, Haddad-derafshi and Tahmasebi (2008)]. Reviewing the literature, it is found that previous investigations generally neglected the effects of the hydrostatic pressure and the residual stress within the actuating membrane when analyzing the pull-in phenomenon in MEMS-based actuator systems. The current study addresses this omission by performing a systematic investigation into the combined effects on the pull-in characteristics of the actuator system of both the hydrostatic pressure acting on the upper surface of the micro circular plate and the residual stress within the plate.

Generally speaking, the dynamic behavior of the nonlinear micro electrostatic actuators is not easily analyzed using traditional methods due to the complexity of the interactions between the electrostatic coupling effects. Accordingly, Han [Han, Rajendran and Atluri (2005)] proposed a Meshless Local Petrov-Galerkin (MLPG) method for solving nonlinear dynamic problems with large deformation and rotations. Lee [Lee, Lin, Lee, Lu, and Liu (2008)] utilized a method based on shifting functions to obtain exact solutions for the large static deflections of beams with nonlinear boundary conditions. Wen [Wen and Hon (2007)] performed meshless computations to analyze the geometrical nonlinearity of Reissner-Mindlin plates.

Differential transformation theory was originally proposed by Zhou in 1986 as a means of solving linear and nonlinear initial value problems in the circuit analysis field [Zhou (1986)]. In more recent years, researchers have applied this theory to the solution of general initial value problems in the mechanical engineering domain [Chiou and Tzeng (1996)]. For example, Chen [Chen and Ho (1996,1998)] utilized differential transformation theory to solve general eigenvalue problems and to analyze the free vibration response of Timoshenko beams. Yu [Yu and Chen (1998,1999)] combined differential transformation theory with the finite difference approximation method to solve the Blasius equation and the nonlinear transient conduction-convection-radiation heat transfer annular fin equation. More recently, Kuo [Kuo and Chen (2003)] employed a hybrid differential transformation / finite difference method to analyze the nonlinear Burgers' equation for the high Reynolds number regime.

In the current study, the hybrid differential transformation / finite difference method is employed to analyze the pull-in phenomenon of the electrostatically-actuated micro circular plate system shown in Fig. 1. In formulating the nonlinear governing equation of the circular plate, explicit account is taken of both the hydrostatic pres-

sure and the residual stress. The validity of the proposed approach is verified by comparing the numerical results obtained for the pull-in voltage with those obtained using two different methodologies presented in the literature. namely the finite difference method (FDM) presented in [Soleymani, Sadeghian, Tahmasebi and Rezazadeh (2006)] and the CoSolve simulation and closed-form model presented in [Osterberg (1995)]).

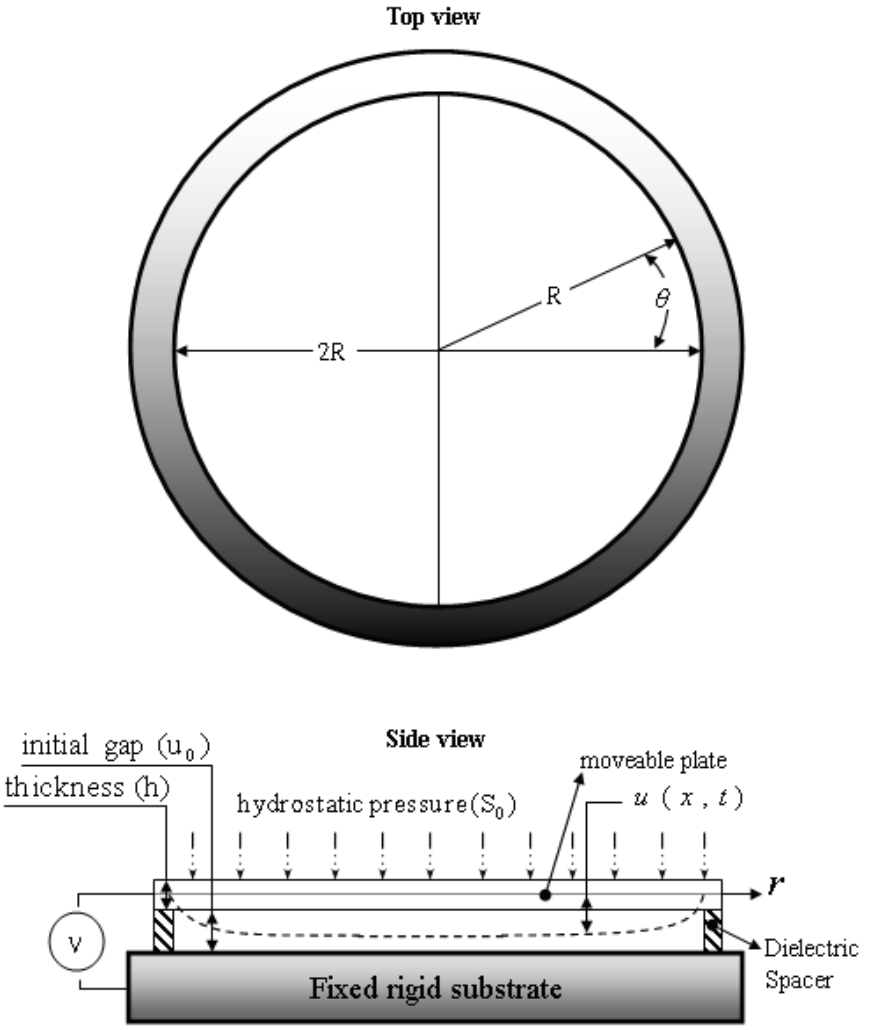

Figure 1: Schematic illustration of micro circular plate actuator system.

2 Differential Transformation Theory

The basic principles of differential transformation theory can be summarized as follows:

Let $y(t)$ be an analytic function in the time domain T. The differential transformation of y at time $t = t_0$ is given by

$$Y(k;t_0) = M(k)\left(\frac{d^k}{dt^k}(q(t)y(t))\right)_{t=t_0}, \quad k \in K, \tag{1}$$

where k belongs to a set of nonnegative integers which collectively comprise the K domain, $Y(k;t_0)$ is the transformed function in the transformation domain, and is known as the spectrum of $y(t)$ at $t = t_0$ in the K domain. $M(k)$ is a weighting factor, and $q(t)$ is a kernel corresponding to $y(t)$. $M(k)$ and $q(t)$ are not both equal to zero and $q(t)$ is an analytic function in the time domain T.

The differential inverse transformation of $Y(k;t_0)$ has the form

$$y(t) = \frac{1}{q(t)}\sum_{k=0}^{\infty}\frac{(t-t_0)^k}{k!}\frac{Y(k;t_0)}{M(k)}, \quad t \in T, \tag{2}$$

Let $M(k)$ and $q(t)$ be given by $M(k) = \frac{H^k}{k!}$ and $q(t) = 1$, respectively, where H is the time interval. At time $t_0 = 0$, Eq. (2) therefore becomes

$$Y(k) = \frac{H^k}{k!}\left[\frac{d^k y(t)}{dt^k}\right]_{t=0}, \quad k \in K, \tag{3}$$

The differential inverse transformation of $Y(k)$ is given by

$$y(t) = \sum_{k=0}^{\infty}\left(\frac{t}{H}\right)^k Y(k), \quad t \in T, \tag{4}$$

Substituting Eq. (3) into Eq. (4) gives

$$y(t) = \sum_{k=0}^{\infty}\frac{t^k}{k!}\left[\frac{d^k y(t)}{dt^k}\right]_{t=0}, \quad t \in T, \tag{5}$$

Equation (5) has the form of a Taylor series expansion. Therefore, the basic operating properties of the differential transform are as follows:

(a) Linearity Operation

$$T[\alpha y(t) + \beta z(t)] = \alpha Y(k) + \beta Z(k), \tag{6}$$

where T denotes the differential transformation operation, and α and β are any real numbers.

(b) Convolution Operation

$$T[y(t)z(t)] = Y(k) \otimes Z(k) = \sum_{\ell=0}^{k} Y(\ell)Z(k-\ell), \tag{7}$$

$$T[y^m(t)] = kY(0)Y^m(k) = \sum_{\ell=1}^{k} [(m+1)\,\ell]\,Y(\ell)Y^m(k-\ell), \quad m \in N, \tag{8}$$

where T denotes the differential transformation operation and $\otimes$ is a convolution operation.

(c) Differential Operation

$$T\left[\frac{d^n y(t)}{dt^n}\right] = \frac{(k+n)!}{k!H^n} Y(k+n), \tag{9}$$

where T denotes the differential transformation operation and n is the order of differentiation [Yu and Chen (1998); Yu and Chen (1999); Kuo and Chen (2003)].

3 Modeling of Micro Circular Plate

In deriving the dynamic governing equation of motion for the micro circular plate shown in Fig. 1, an assumption is made that the plate is subject to small strains and displacements and undergoes an axi-symmetric bending effect. The governing equation is normalized for analytical convenience and is then solved using the hybrid differential transformation / finite difference approximation method.

3.1 Governing equation of micro circular plate

As shown in Fig. 1, the micro-actuator system considered in this study comprises a movable circular plate with a thickness h attached at its perimeter to a fixed rigid substrate. The gap between the two plates is filled with air and has an initial height of u_0. The application of an external voltage across the two electrodes creates an electrostatic attractive force which causes the micro circular plate to deflect in the downward direction toward the lower substrate. The displacement u of the circular plate is assumed to vary as a function of both the radial position r and the time t, i.e. $u = u(r,t)$. Assuming that the effects of the hydrostatic pressure and residual stress are ignored, the dynamic governing equation of motion of the micro circular

plate can be expressed in a polar coordinate form as follows [Nayfeh and Younis (2004)]:

$$\rho h\frac{\partial^2 u}{\partial t^2}+D\left(\frac{\partial^2}{\partial r^2}+\frac{1}{r}\frac{\partial}{\partial r}+\frac{1}{r^2}\frac{\partial}{\partial \theta}\right)\left(\frac{\partial^2 u}{\partial r^2}+\frac{1}{r}\frac{\partial u}{\partial r}+\frac{1}{r^2}\frac{\partial u^2}{\partial \theta}\right)=f(r), \tag{10}$$

where ρ is the density of the micro circular plate, u is the deflection of the micro circular plate at a distance r from the center of the plate, D is the flexural rigidity of the plate and $f(r)$ is the electrostatic force acting between the two electrodes. D and $f(r)$ can be expressed respectively as

$$D=\frac{Eh^3}{12(1-\upsilon^2)}, \tag{11}$$

$$f(r)=\frac{\varepsilon_0 V^2}{2(u_0-u)^2}, \tag{12}$$

where ε_0, V and u_0 represent the permittivity of free space, the voltage between the upper and lower electrodes, and the initial gap height between the electrodes, respectively. Furthermore, E, h and υ are the Young's modulus, thickness and Poisson ratio of the micro circular plate, respectively.

However, due to the small physical size of the MEMS actuator system shown in Fig.1, it is essential to take the effects of hydrostatic pressure and residual stress into account when modeling the pull-in phenomenon. It is supposed that the symmetry deflection of the micro circular plate is irrelevant to polar coordinate θ. Thus, the dynamic governing equation given in Eq. 10 should be rewritten as follows:

$$\rho A\frac{\partial^2 u}{\partial t^2}+D\left(\frac{\partial^2}{\partial r^2}+\frac{1}{r}\frac{\partial}{\partial r}\right)\left(\frac{\partial^2 u}{\partial r^2}+\frac{1}{r}\frac{\partial u}{\partial r}\right)-T_r\left(\frac{\partial^2 u}{\partial r^2}+\frac{1}{r}\frac{\partial u}{\partial r}\right) = \frac{\varepsilon_0 V^2}{2(u_0-u)^2}+S_0, \tag{13}$$

where T_r is the residual force [Osterberg and Senturia (1997)] and S_0 is the hydrostatic pressure which acts on the upper surface of the plate and contributes to the effects of the electrostatic force in causing the plate to deflect toward the lower substrate.

The boundary conditions for Eq. (13) are as follows:

$$u(r,t)=\frac{\partial u(r,t)}{\partial r}=0, \quad \text{at } r=0$$

$$u(r,t)=\frac{\partial u(r,t)}{\partial r}=0, \quad \text{at } r=\pm R \tag{14}$$

where R denotes the radius of the circular plate.

Meanwhile, the initial conditions are given by:

$$u(r,0) = \frac{\partial u(r,0)}{\partial t} = 0. \tag{15}$$

3.2 Normalized governing equation

For analytical convenience, the displacement term u in the governing equation is normalized with respect to the initial gap height between the plates, Similarly, the radial position term r is normalized with respect to the plate radius, and the time term t is normalized with respect to the constant T_1, i.e.

$$u^* = \frac{u}{u_0}, \quad r^* = \frac{r}{R}, \quad t^* = \frac{t}{T_1}, \tag{16}$$

where $T_1 = \sqrt{\frac{\rho h R^4}{D}}$.

In addition, the voltage, residual stress and hydrostatic pressure terms are normalized as follows:

$$V^* = \sqrt{\frac{\varepsilon_0 R^4 V^2}{2Du_0^3}}, \quad T_r^* = \frac{T_r R^2}{D} \quad S_0^* = \frac{S_0 R^4}{Du_0}, \tag{17}$$

Substituting Eqs. (16) and (17) into Eqs. (13)–(15), the normalized governing equation can be expressed as follows:

$$\frac{\partial^2 u^*}{\partial t^{*2}} + \frac{\partial^4 u^*}{\partial r^{*4}} + \frac{2}{r^*}\frac{\partial^3 u^*}{\partial r^{*3}} - \frac{1}{r^{*2}}\frac{\partial^2 u^*}{\partial r^{*2}} + \frac{1}{r^{*3}}\frac{\partial u^*}{\partial r^*} - T_r^*\frac{\partial^2 u^*}{\partial r^{*2}} - T_r^*\frac{1}{r^*}\frac{\partial u^*}{\partial r^*} = \frac{V^{*2}}{(1-u^*)^2} + S_0^*; \tag{18}$$

The corresponding boundary conditions are given as

$$u^*(r^*,t^*) = \frac{\partial u^*(r^*,t^*)}{\partial r^*}0, \quad \text{at } r^* = 0$$

$$u^*(r^*,t^*) = \frac{\partial u^*(r^*,t^*)}{\partial r^*} = 0, \quad \text{at } r^* = 1 \tag{19}$$

The initial condition is given by

$$u^*(r^*,0) = \frac{\partial u^*(r^*,0)}{\partial t^*} = 0, \tag{20}$$

The nonlinear electrostatic force term $\frac{V^{*2}}{(1-u^*)^2}$ in Eq. (18) can be approximated via the following Taylor expansion series:

$$\frac{V^{*2}}{(1-u^*)^2} = V^{*2}\left(1+2u^*+3u^{*2}+4u^{*3}+5u^{*4}\cdots\cdots\right), \tag{21}$$

Neglecting the higher-order terms, and substituting Eq. (21) into Eq. (18), the nonlinear governing equation of the micro circular plate subject to the combined effects of electrostatic force, hydrostatic pressure and residual stress can be expressed as

$$\frac{\partial^2 u^*}{\partial t^{*2}} + \frac{\partial^4 u^*}{\partial r^{*4}} + \frac{2}{r^*}\frac{\partial^3 u^*}{\partial r^{*3}} - \frac{1}{r^{*2}}\frac{\partial^2 u^*}{\partial r^{*2}} + \frac{1}{r^{*3}}\frac{\partial u^*}{\partial r^*} - T_r^*\frac{\partial^2 u^*}{\partial r^{*2}} - T_r^*\frac{1}{r^*}\frac{\partial u^*}{\partial r^*}$$
$$= V^{*2}\left(1+2u^*+3u^{*2}+4u^{*3}+5u^{*4}\right) + S_0^*, \tag{22}$$

3.3 Application of hybrid method to solution of governing equation

In this section, the normalized governing equation given in Eq. (22), and the corresponding boundary conditions and initial condition given in Eqs. (19) and (20), respectively, are solved using the hybrid differential transformation / finite difference method. The solution procedure commences by applying the differential transformation process with respect to the time domain t to each term in the governing equation, i.e.

$$T\left[\frac{\partial^2 u^*}{\partial t^{*2}}\right] = \frac{(k+1)(k+2)}{H^2}U(r^*,k+2),$$

$$T\left[\frac{\partial^4 u^*}{\partial r^{*4}}\right] = \frac{d^4U(r^*,k)}{dr^{*4}},$$

$$T\left[\frac{2}{r^*}\frac{\partial^3 u^*}{\partial r^{*3}}\right] = \frac{2}{r^*}\frac{d^3U(r^*,k)}{dr^{*3}},$$

$$T\left[\frac{1}{r^{*2}}\frac{\partial^2 u^*}{\partial r^{*2}}\right] = \frac{1}{r^{*2}}\frac{d^2U(r^*,k)}{dr^{*2}},$$

$$T\left[\frac{1}{r^{*3}}\frac{\partial u^*}{\partial r^*}\right] = \frac{1}{r^{*3}}\frac{dU(r^*,k)}{dr^*},$$

$$T\left[T_r^*\frac{\partial^2 u^*}{\partial r^{*2}}\right] = T_r^*\frac{d^2U(r^*,k)}{dr^{*2}},$$

$$T\left[T_r^*\frac{1}{r^*}\frac{\partial u^*}{\partial r^*}\right] = T_r^*\frac{1}{r^*}\frac{dU(r^*,k)}{dr^*},$$

$$T\left[2V^{*2}u^{*2}\right] = 2V^{*2}U(r^*,k),$$

$$T\left[3V^{*2}u^{*2}\right] = 3V^{*2}\left(U(r^*,k)\otimes U(r^*,k)\right) = 3V^{*2}\left(\sum_{\ell=0}^{k} U(r^*,\ell)U(r^*,k-\ell)\right),$$

$$T\left[4V^{*2}u^{*3}\right] = 4V^{*2}\left(\sum_{\ell=1}^{k} [(3+1)\ell-k]U(r^*,\ell)U^3(r^*,k-\ell)\right),$$

$$T\left[5V^{*2}u^{*4}\right] = 5V^{*2}\left(\sum_{\ell=1}^{k} [(4+1)\ell-k]U(r^*,\ell)U^4(r^*,k-\ell)\right),$$

$$T\left[V^{*2}\right] = V^{*2}\delta(k),$$

$$T[S_0^*] = S_0^*\delta(k). \tag{23}$$

Note that $\delta(k)$ is specified as

$$\delta(k) = \begin{cases} 1, & \text{for } k=0 \\ 0 & \text{otherwise} \end{cases}$$

Thus, Eq. (22) can be rewritten as follows:

$$\frac{(k+1)(k+2)}{H^2}U(r^*,k+2) + \frac{d^4U(r^*,k)}{dr^{*4}} + \frac{2}{r^*}\frac{d^3U(r^*,k)}{dr^{*3}} - \frac{1}{r^{*2}}\frac{d^2U(r^*,k)}{dr^{*2}}$$
$$+\frac{1}{r^{*3}}\frac{dU(r^*,k)}{dr^*} - T_r^*\frac{d^2U(r^*,k)}{dr^{*2}} - T_r^*\frac{1}{r^*}\frac{dU(r^*,k)}{dr^*} = V^{*2}\delta(k) + 2V^{*2}U(r^*,k)$$
$$+3V^{*2}\left(\sum_{\ell=0}^{k} U(r^*,\ell)U(r^*,k-\ell)\right) + 4V^{*2}\left(\sum_{\ell=1}^{k} [(3+1)\ell-k]U(r^*,\ell)U^3(r^*,k-\ell)\right)$$
$$+5V^{*2}\left(\sum_{\ell=1}^{k} [(4+1)\ell-k]U(r^*,\ell)U^4(r^*,k-\ell)\right) + S_0^*\delta(k), \tag{24}$$

Similarly, the boundary conditions can be rewritten as

$$T[u^*(r^*,t^*)] = U(r^*,k) = 0, \quad \text{at } r^* = 0$$

$$T\left[\frac{\partial u^*(r^*,t^*)}{\partial r^*}\right] = \frac{dU(r^*,k)}{dr^*} = 0, \quad \text{at } r^* = 0$$

$$T[u^*(r^*,t^*)] = U(r^*,k) = 0, \quad \text{at } r^* = 1$$

$$T\left[\frac{\partial u^*(r^*,t^*)}{\partial r^*}\right] = \frac{dU(r^*,k)}{dr^*} = 0, \quad \text{at } r^* = 1 \tag{25}$$

Finally, the initial conditions can be rewritten as

$$T[u^*(r^*,0)] = U(r^*,0) = 0\ ,\ k = 0$$

$$T\left[\frac{\partial u^*(r^*,0)}{\partial t^*}\right] = \frac{k+1}{H}U(r^*,k+1) = 0\ ,\ k = 0 \tag{26}$$

where $U(r^*,k)$ is the spectrum of $u^*(r^*,t^*)$, k and ℓ are transformation parameters, and H is the time interval.

In the second stage of the solution procedure, the finite difference approximation method is applied with respect to r^* to the transformed versions of the equation of motion, boundary conditions and initial conditions given in Eqs. (24), (25) and (26), respectively.

Applying the fourth-order accurate central difference scheme, Eq. (24) can be expressed as follows:

$$\begin{aligned}
&\frac{(k+1)(k+2)}{H^2}U_i(k+2) + \frac{U_{i+2}(k) - 4U_{i+1}(k) + 6U_i(k) - 4U_{i-1}(k) + U_{i-2}(k)}{\Delta r^{*4}} \\
&+ \frac{1}{r^{*3}_i}\frac{U_{i+1}(k) - U_{i-1}(k)}{2\Delta r^*} \\
&- \frac{1}{r^{*2}_i}\frac{U_{i+1}(k) - 2U_i(k) + U_{i-1}(k)}{\Delta r^{*2}} + \frac{2}{r^*_i}\frac{U_{i+2}(k) - 2U_{i+1}(k) + 2U_{i-1}(k) - U_{i-2}(k)}{2\Delta r^{*3}} \\
&- T^*_r\frac{U_{i+1}(k) - 2U_i(k) + U_{i-1}(k)}{\Delta r^{*2}} - T^*_r\frac{1}{r^*_i}\frac{U_{i+1}(k) - U_{i-1}(k)}{2\Delta r^*} = V^{*2}\delta(k) + 2V^{*2}U_i(k) \\
&+ 3V^{*2}\left(\sum_{\ell=0}^{k} U_i(\ell)U_i(k-\ell)\right) + 4V^{*2}\left(\sum_{\ell=1}^{k}\left[(3+1)\ell - k\right]U_i(\ell)U_i^3(k-\ell)\right) \\
&+ 5V^{*2}\left(\sum_{\ell=1}^{k}\left[(4+1)\ell - k\right]U_i(\ell)U_i^4(k-\ell)\right) + S^*_0\delta(k),
\end{aligned} \tag{27}$$

where Δr^* is the radius interval and i is a position index in the r direction. In Eq.

(27), $U_i(k+2)$ is the only unknown, and can therefore be derived as follows:

$$
\begin{aligned}
U_i(k+2) = {} & \frac{H^2}{(k+1)(k+2)} \times \\
& \left[V^{*2}\delta(k) + 2V^{*2}U_i(k) + 3V^{*2}\left(\sum_{\ell=0}^{k} U_i(\ell)U_i(k-\ell)\right)\right. \\
& + 4V^{*2}\left(\sum_{\ell=1}^{k}[(3+1)\ell - k]U_i(\ell)U_i^3(k-\ell)\right) \\
& + 5V^{*2}\left(\sum_{\ell=1}^{k}[(4+1)\ell - k]U_i(\ell)U_i^4(k-\ell)\right) \\
& + S_0^*\delta(k) - \frac{1}{r_i^{*3}}\frac{U_{i+1}(k) - U_{i-1}(k)}{2\Delta r^*} \\
& - \frac{U_{i+2}(k) - 4U_{i+1}(k) + 6U_i(k) - 4U_{i-1}(k) + U_{i-2}(k)}{\Delta r^{*4}} \\
& + \frac{1}{r_i^{*2}}\frac{U_{i+1}(k) - 2U_i(k) + U_{i-1}(k)}{\Delta r^{*2}} \\
& - \frac{2}{r_i^*}\frac{U_{i+2}(k) - 2U_{i+1}(k) + 2U_{i-1}(k) - U_{i-2}(k)}{2\Delta r^{*3}} + T_r^*\frac{U_{i+1}(k) - 2U_i(k) + U_{i-1}(k)}{\Delta r^{*2}} \\
& \left. + T_r^*\frac{1}{r_i^*}\frac{U_{i+1}(k) - U_{i-1}(k)}{2\Delta r^*}\right], \qquad (28)
\end{aligned}
$$

Applying the first-order accurate central difference scheme to Eq. (25), the boundary conditions can be expressed as

$$
\begin{aligned}
& U_i(k) = 0, \\
& \frac{U_{i+1}(k) - U_{i-1}(k)}{2\Delta r^*} = 0, \\
& U_j(k) = 0, \\
& \frac{U_{j+1}(k) - U_{j-1}(k)}{2\Delta r^*} = 0, \qquad (29)
\end{aligned}
$$

where j indicates the final index position in the $r$direction.

Similarly, the initial condition can be derived as

$$
\begin{aligned}
& U_i(0) = 0, \\
& \frac{1}{H}U_i(1) = 0 \ \rightarrow U_i(1) = 0, \qquad (30)
\end{aligned}
$$

4 Numerical Results and Discussion

To confirm the validity of the hybrid solution procedure described in Section 3, the numerical results obtained for the pull-in voltage of the micro circular plate shown in Fig. 1 in the absence of hydrostatic and residual stress effects are compared with those calculated using two methods presented in the literature, namely the CoSolve simulation model and the 2-D closed-form solution procedure (both presented in [Osterberg (1995)]). In performing the analysis, the material and geometry parameters of the micro circular plate are assigned the values shown in Table 1. The comparative results for the pull-in voltage are presented in Table 2. As shown, the pull-in voltage computed using the proposed hybrid method deviates by just 0.2% and 1.75% from the CoSolve and closed-form solutions, respectively.

Table 1: Material and geometry parameters of micro circular plate.

Parameters	Value
Young's modulus (E) (GPa)	169
Poisson's Ratio (ν)	0.3
Density (ρ) (Kg/m^3)	2.33×10^3
Permittivity of free space (ε_0) (F/m)	8.8541878×10^{-12}
Thickness of the micro circular plate (h) (μm)	20
Initial gap (μ_0) (μm)	1
Radius of the plate (R) (μm)	250

Table 2: Comparison of pull-in voltage results obtained using hybrid method and two methods presented in the literature, respectively. (Note that the effects of residual stress and hydrostatic pressure are neglected in every case.)

	Hybrid Method (H.M)	CoSolve Simulation [Osterberg (1995)]	2D closed Form [Osterberg (1995)]	Deviation 1* (%)	Deviation 2** (%)
Pull-in Voltage (V)	319.5	319	314	0.2	1.75

$$*\text{Deviation 1} = \left| \frac{\text{(Cosolve Simulation - H.M)}}{\text{Cosolve Simulation}} \times 100\% \right|$$

$$**\text{Deviation 2} = \left| \frac{\text{(2D close Form - H.M)}}{\text{2D closed Form}} \times 100\% \right|$$

Table 3: Variation of calculated pull-in voltage with residual stress as computed by current method and finite difference method (FDM), respectively. (Note that effects of hydrostatic pressure are neglected.)

Residual Stress (Mpa)	Pull-in Voltage (V)		$(\%)^*$
	Hybrid Method (H.M)	F.D.M [Soleymani *et al.* (2006)]	
-20	317.9	313.37	1.45
0	319.5	315.51	1.26
40	322.8	319.73	0.96

$$*\Delta = \left| \frac{\text{(F.D.M - H.M)}}{\text{F.D.M}} \times 100\% \right|$$

Table 3 compares the pull-in voltage values obtained from the hybrid method and the finite difference method (FDM) presented in [Osterberg (1995)] when the effects of the residual stress are taken into account. (Note that the effects of the hydrostatic pressure acting on the upper surface of the plate are ignored.) For both models, it is observed that the pull-in voltage increases with an increasing value of the residual stress. This is to be expected since the positive residual stress acts in the opposite direction to the attractive electrostatic force. Consequently, a greater electrostatic force (i.e. a higher external voltage) must be applied before the upper plate collapses and makes contact with the lower substrate. Table 3 shows that the solutions obtained using the hybrid method deviate by no more than 1.45% from those calculated using the FDM method. Thus, the validity of the proposed method for analyzing the behavior of the micro circular actuator plate is confirmed.

Figure 2 illustrates the variation of the dimensionless plate deflection with the hydrostatic pressure as a function of the applied voltage. (Note that the effects of residual stress are ignored.) The results show that for each value of the applied voltage, the circular plate becomes unstable at a certain critical value of the hydrostatic pressure and then collapses, causing the center of the plate to make transient contact with the lower substrate. As expected, the magnitude of the pull-in hydrostatic pressure reduces as the value of the externally applied voltage increases.

Figure 3 illustrates the variation of the micro plate deflection in the radial direction as a function of the applied voltage. (Note that the effects of the residual stress and hydrostatic pressure are both ignored.) The results show that at voltages lower than the pull-in voltage, the micro plate deflects symmetrically about its center point. As expected, the deflection of the micro plate increases with an increasing voltage. Furthermore, it is observed that the pull-in voltage has a theoretical value of 319.5

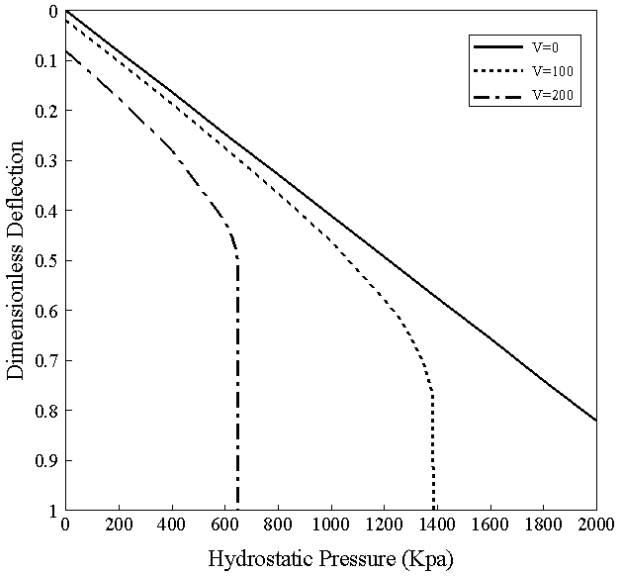

Figure 2: Variation of dimensionless deflection with hydrostatic pressure as function of applied voltage. (Note that effects of residual stress are neglected.)

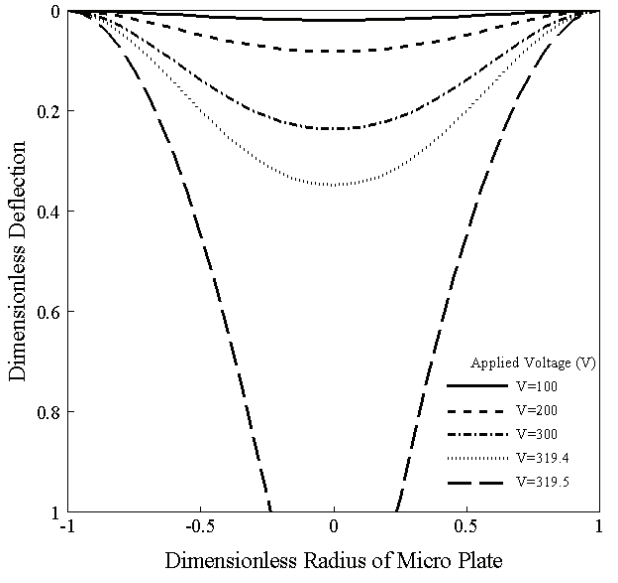

Figure 3: Variation of dimensionless deflection with dimensionless radius of circular plate as function of applied voltage. (Note that effects of both residual stress and hydrostatic pressure are neglected.)

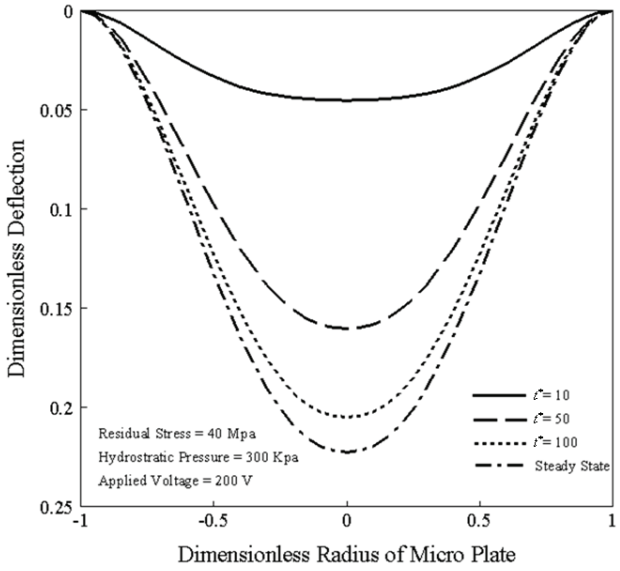

Figure 4: Variation of dimensionless deflection with dimensionless radius of circular plate as function of dimensionless time.

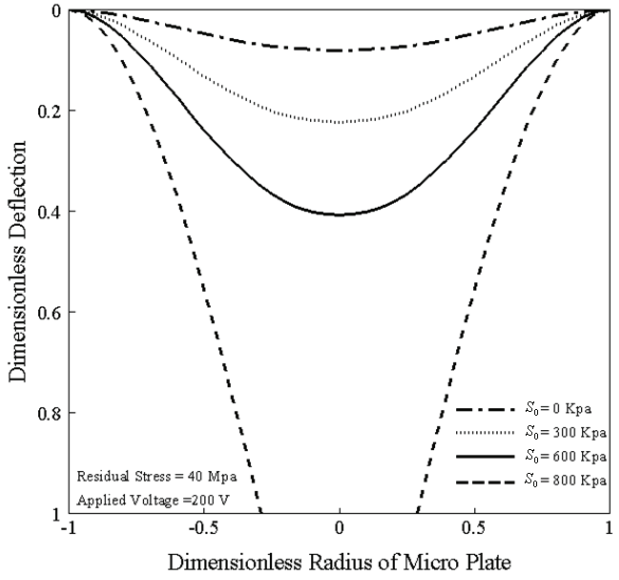

Figure 5: Variation of dimensionless deflection with dimensionless radius of circular plate as function of hydrostatic pressure. (Note: residual stress = 40 MPa and applied voltage = 200 V.)

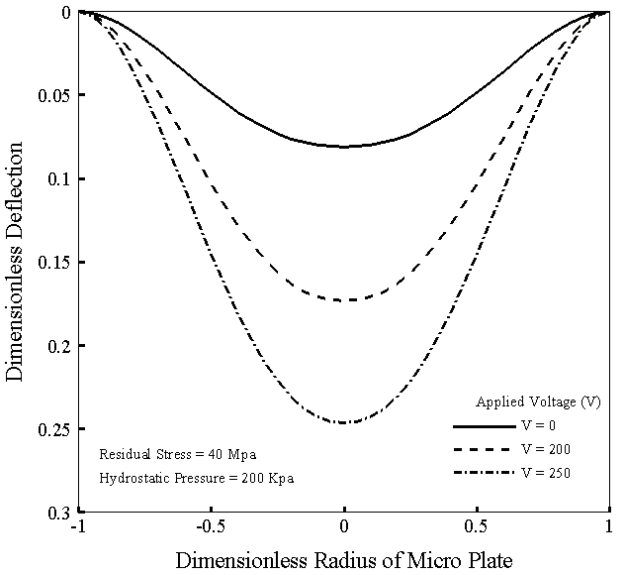

Figure 6: Variation of dimensionless deflection with dimensionless radius of circular plate as function of applied voltage. (Note: residual stress = 40 MPa and applied hydrostatic pressure = 200 KPa.)

V for the micro plate parameters considered in Table 1.

Figures 4, 5 and 6 illustrate the variation of the micro-plate deflection in the radial direction under various residual stress and hydrostatic pressure conditions. Figure 4 shows the evolution of the micro-plate deflection over time for the case of an applied voltage of 200 V, a residual stress of 40 MPa and a hydrostatic pressure of 300 kPa. The results confirm that the maximum point of deflection occurs at the center of the micro circular plate. Furthermore, since the magnitude of the applied voltage is lower than the pull-in voltage, the micro plate attains an equilibrium displacement condition in the steady state. Figure 5 illustrates the effect on the micro plate displacement of an increasing hydrostatic pressure given a constant applied voltage of 200 V. The results show that the deflection of the micro plate increases with an increasing hydrostatic pressure over the range $S_0 = 0 \sim 600$ kPa. However, when the hydrostatic pressure is increased to 800 kPa, the combined effects of the electrostatic force and hydrostatic pressure acting in the downward direction overcome the resistive effect of the restoring force, and thus the plate collapses.

Finally, Fig. 6 shows the effect of the applied voltage on the micro plate deflection

for a constant residual stress of 40 MPa and a constant hydrostatic pressure of 200 kPa. As expected, the deflection of the center point of the plate increases with an increasing applied voltage. However, the pull-in phenomenon does not occur since the combined effect of the constant hydrostatic pressure and the electrostatic force generated by voltages in the range 0∼250 V is insufficient to overcome the restoring force developed within the circular plate.

5 Conclusions

This study has utilized a hybrid differential transformation / finite difference approximation method to analyze the pull-in phenomenon of a MEMS-based electrostatic actuator system comprising a thin micro circular plate and a lower fixed electrode. In contrast to previous studies, the governing equation developed in this study takes into account the effects of both the hydrostatic force acting on the upper surface of the circular plate and the residual stress within the plate itself. The validity of the proposed hybrid method has been confirmed by comparing the solutions obtained for the pull-in voltage with those obtained using two methodologies presented in the literature (i.e. the finite difference method (FDM) presented in [Soleymani, Sadeghian, Tahmasebi and Rezazadeh (2006)] and the CoSolve simulations and closed-form model presented in [Osterberg (1995)]).

The results have shown that the hybrid method successfully captures the respective effects of the applied voltage, residual stress and hydrostatic pressure in determining the onset of the pull-in phenomenon within the actuator system. As expected, the pull-in voltage increases with an increasing residual stress, but reduces with an increasing hydrostatic pressure. The maximum deviation between the pull-in voltage calculated using the hybrid method and the solutions obtained using the methodologies presented in the literature is just 1.75%, and thus the validity of the proposed approach is confirmed.

In a future study, the hybrid method presented in this study will be extended to analyze the more complex case in which the air between the micro circular plate and the lower substrate exerts a damping effect which opposes the motion of the micro plate as it deflects in the downward direction.

Acknowledgement: The authors gratefully acknowledge the financial support provided to this study by the National Science Council of Taiwan under Grant Number NSC-96-2221-E006-171-MY2.

Reference

Bettini, P.; Brusa, E.; Munteanu, M.; Specogna, R.; Trevisan F. (2008): Innovative NumericalMethods for NonlinearMEMS: the Non-Incremental FEM vs. the Discrete Geometric Approach. *CMES: Computer Modeling in Engineering & Sciences*, vol. 33, no. 3, pp. 111-120.

Bustgens, B.; Bacher, W.; Menz, W.; Schomburg, W. K. (1994): Micropump manufactured by thermoplastic molding. *IEEE Micro Electra Mechanical Systems Workshop*, Oiso, Japan, pp. 18-21.

Chen, C.K.; Ho, S.H. (1996): Application of differential transformation to eigenvalue problem. *Applied mathematics and computation*, vol. 79, pp. 173-188.

Chen, C.K.; Ho, S.H. (1998): Free vibration analysis of non-uniform Timoshenko beams using differential transform, *Applied mathematical modeling*, vol. 22, pp. 231-250.

Chiou, J.S.; Tzeng, J.R. (1996): Application of the Taylor transform to nonlinear vibration problems. *ASME, J. Vibration and Acoustics*, vol. 118, pp. 83-87.

Duan, D.; Wan, Kai-Tak (2007): Analysis of One-Dimensional and Two-Dimensional Thin Film "Pull-in" Phenomena Under the Influence of an Electrostatic Potential. *ASME J.Appl. Mech.*, vol. 74, pp. 927-934.

Han, Z.D.; Rajendran, A.M.; Atluri, S.N. (2005): Meshless Local Petrov-Galerkin (MLPG) Approaches for Solving Nonlinear Problems with Large Deformations and Rotations. *CMES: Computer Modeling in Engineering & Sciences*, vol. 10, no. 1, pp. 1–12.

Hu, M.; Du, H.; Ling, S.; Liu, B.; Lau, G. (2005): Fabrication of a rotary micromirror for fiber-optic switching. *Microsyst Technol*, vol. 11 ,pp. 987–990.

Kuo, B. L.; Chen, C.K. (2003): Application of the Hybrid Method to the Solution of the Nonlinear Burgers' Equation. *ASME J. Appl. Mech.*, vol. 70, pp. 926–929.

Lee, S.Y.; Lin, S.M.; Lee, C.S.; Lu, S.Y.; Liu, Y.T. (2008): Exact large deflection of beams with nonlinear boundary conditions. *CMES: Computer Modeling in Engineering & Sciences*, vol. 30, no. 1, pp. 27–36.

Luharuka, R.; LeBlanc, S.; Bintoro, J. S.; Berthelot, Y. H.; B., Hesketh, P. J. (2008): Simulated and experimental dynamic response characterization of an electromagnetic microvalve. *Sensors and Actuators A*, vol. 143, pp. 399-408.

Nabian, A.; Rezazadeh, G.; Haddad-derafshi, M.; Tohmasebi, A. (2008): Mechanical behavior of a circular micro plate subjected to uniform hydrostatic and non-uniform electrostatic pressure. *Microsyst Technol*, vol. 14, pp. 235–240.

Nayfeh, A.H.; Younis, M.I. (2004): A new approach to the modeling and sim-

ulation of flexible microstructures under the effect of squeeze-film damping. *J. Micromech. Microeng.*, vol. 14, pp. 170-181.

Osterberg, P.M. (1995): Electrostatically actuated microelectromechancial test structures for material property measurement. Ph.D. dissertation, *Mass. Instit. Tech.*, Cambridge, MA.

Osterberg, P.M.; Senturia, S.D. (1997): M-test: A test chip for MEMS material property measurement using electrostatically actuated test structures. *Journal of Microelectromechanical System*, vol. 6, no. 2, pp. 107–118.

Rezazadeh, G.; Tahmasebi, A.; Zubstov, M. (2006): Application of piezoelectric layers in electrostatic MEM actuators: controlling of pull-in voltage. *Microsyst Technol*, vol. 12, pp. 1163–1170.

Soleymani, P.; Sadeghian, H.; Tahmasebi, A.; Rezazadeh, G. (2006): Pull-in Instability Investigation of Circular Micro Pump Subjected to Nonlinear Electrostatic Force. *Sensors & Transducers Journal*, vol. 69, no. 7, pp. 622-628.

Son, I.; Lal, A.; Hubbard, B.; Olsen, T. (2001): A multifunctional silicon-based microscale surgical system. *Sensors and Actuators A*, vol. 91, pp. 351-356.

Wang, Q.X.; Li, Hua.; Lam, K.Y. (2007): Analysis of microelectromechanical systems (MEMS) devices by the meshless point weighted least-squares method. *Comput. Mech.*, vol. 40, pp. 1-11.

Wen, P.H.; Hon, Y.C. (2007): Geometrically nonlinear analysis of reissnermindlin plate by meshless computation. *CMES: Computer Modeling in Engineering & Sciences*, vol. 21, no. 3, pp. 177–191.

Ye, W.; Mukherjee, S. (2000): Design and fabrication of an electrostatic variable gap comb drive in micro-electromechanical systems. *CMES: Computer Modeling in Engineering & Sciences*, vol. 1, no. 1, pp. 111-120.

Yu, L.T.; Chen, C.K. (1998): The solution of the Blasius equation by the differential transformation method. *Math. Comput. Modeling*, vol. 28, no. 1, pp. 101–111.

Yu, L.T.; Chen, C.K. (1999): Application of the Hybrid Method to the Transient Thermal Stresses Response in Isotropic Annular Fins. *ASME J. Appl. Mech.*, vol. 66, pp. 340–346.

Zhou, X. (1986): Differential Transformation and Its Applications for Electrical Circuits. *Huazhong University Press*, Wuhan, China. (in Chinese)